Particle Morphology for Polyolefins Synthesized With Supported Metallocene Catalysts

S. D. NAIK, W. H. RAY

Department of Chemical Engineering, University of Wisconsin, Madison, Wisconsin 53706

Received 28 January 2000; accepted 29 May 2000

ABSTRACT: A detailed model describing particle growth and morphology in polyolefins synthesized using supported metallocene catalysts is presented. The multigrain model (MGM) is extended to consider metal extraction and the effects of polymer particle compressibility, in addition to monomer sorption and mass and heat transfer considerations. The effects of active metal extraction into the polymer phase and the pores of the particle on the kinetics of polymerization and morphological features of the polymer particle are studied. The effects of greater compressibility of polymer particles on morphological features such as particle porosity are studied. Model predictions for porosity and morphology are shown to reproduce similar trends as have been reported in experimental studies. © 2001 John Wiley & Sons, Inc. J Appl Polym Sci 79: 2565–2579, 2001

INTRODUCTION

Traditionally, polyolefins are synthesized using supported Ziegler–Natta catalysts such as $TiCl_4$ or Cr oxide chemically bound to support particles. Emerging technology in olefin polymerization using metallocene or other single-site catalysts enables the synthesis of homo- and copolymers with narrow molecular weight distributions (MWD), narrow chemical compositional distributions (CCD), and better semicrystalline polymer properties. Because most existing processes for olefin polymerization use supported catalysts, the heterogenization of the metallocene catalysts (by supporting it on a suitable support) is often crucial to their adaptation to commercial technology. Thus, the use of supported metallocenes makes it possible to retain the same reactor/process configurations as are in use in current technology using supported Ziegler–Natta catalysts. However, it has been reported widely that the particle morphology of polyolefins obtained from supported metallocenes differs greatly from those obtained under the same conditions using traditional Ziegler–Natta catalysts. For example, it has been observed that the porosity of polymer particles obtained from supported metallocenes is much lower than the porosities obtained with traditional Ziegler–Natta catalysts.[1,2] Lower melting points at similar density and crystallinity levels and smaller crystallite sizes have also been observed with the metallocenes. Some of the observed features in the morphology of metallocene catalyzed polyolefin particles can be explained by considering the mobility of the active metal due to extraction into the polymer phase from the support structure. As discussed later, in slurry systems, the possibility of polymerization in the pores caused by the extracted metal can lead to low porosities.

Polymer particles synthesized using metallocenes have a lower melting point at the same density and crystallinity and are believed to possess less stable crystalline lamellae. Thus, during the growth of the polymer particle, the forces of outward growth can lead to a greater degree of

Correspondence to: W. H. Ray.

Journal of Applied Polymer Science, Vol. 79, 2565–2579 (2001)

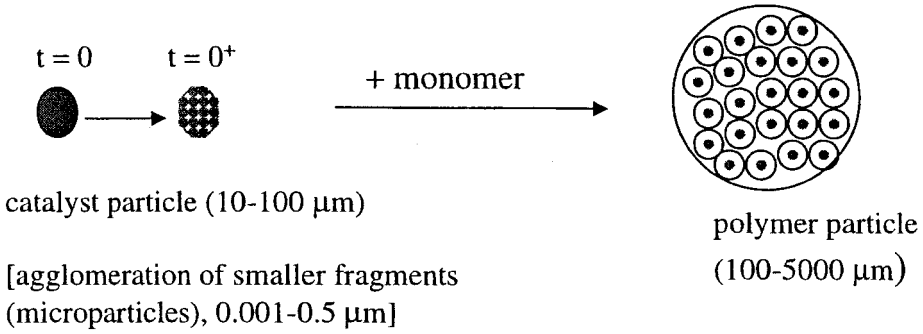

Figure 1 Schematic of polymer growth in polyolefin synthesis.

compression of the softer polymer particles as compared with polymer particles synthesized using tradition supported Ziegler–Natta catalysts. Thus, it can be hypothesized that another plausible reason for the lowered porosity, especially in gas phase systems where there is usually no metal extraction into the pores, is the greater degree of compressibility of the porous polymer particles under reaction conditions.

Here a detailed model of polyolefin particle technology, applicable to both slurry and gas phase reactors, is developed for prediction of these distinctive features observed in supported metallocene systems. The effects of metal extraction with possible polymerization in the pores of the polymer particle and of softer polymer particles on the kinetics and the morphology of the polyolefin particles are studied. The morphological features observed with supported metallocene catalysts are simulated by extending the framework of the multigrain model (MGM), which has been previously used for modeling polyolefin particle morphology using Ziegler–Natta catalysts.[3–7]

POLYMERIC PARTICLE MODEL

Various models have been developed to model the particle morphology of a growing polymer particle for supported Ziegler–Natta catalysts, where the active metal for the catalyst sites is chemically bound to the support. The general picture may be seen in Figure 1, where the catalyst particle fractures as polymerization begins, but the catalyst fragments remain "glued" together by the polymer produced. These catalyst fragments and resulting polymer becomes a polymer particle whose shape and initial morphology are determined by the shape and morphology of the original catalyst support as well as by the manner of catalyst particle breakup. Gentle breakup and controlled particle temperature are desirable for the best morphology; thus, prepolymerization of highly active catalyst particles is often employed.

The MGM is one of the most extensively used models for the prediction of polyolefin particle morphology[3,4,6,7] and is well supported with experimental evidence from electron microscope and TEM studies.[8–13] The model assumes instantaneous fragmentation of the catalyst particle into a large number of catalyst fragments that remain encapsulated by growing polymer to form microparticles. These microparticles are the building blocks of the entire polymer particle, termed the macroparticle. Detailed studies on the effect of mass and heat transport resistance for typical reaction conditions in liquid and gas phase systems using typical Ziegler–Natta catalysts have been previously reported.[6,7,14–18] The MGM models the transport of mass across the external boundary layer of the macroparticle as well as mass transport through the pores of the macroparticle (i.e., in the voids between the microparticles). Diffusion limitations in the pores can lead to concentration gradients of species such as monomers, cocatalyst, and donor. At every radius of the macroparticle, sorption equilibrium is assumed for the monomer and other species at the outer surface of the microparticles. This is followed by diffusion of these species through the semicrystalline polymer of the microparticles to catalyst sites located on the catalyst fragment. In a typical Ziegler–Natta supported catalyst, all reactions occur on the surface of the catalyst fragments inside the microparticles. The particle en-

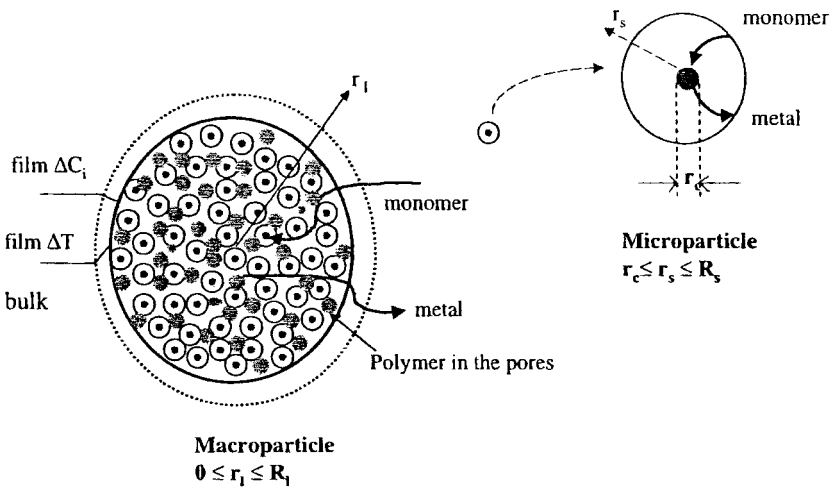

Figure 2 Schematic of multigrain model, with metal extraction.

ergy balance is similar, except that heat is transported out from the catalyst fragment where the large heat of reaction is released, across the radius of the microparticle, through the pores and polymer at every radius of the macroparticle, and through the macroparticle boundary layer. Convective transport of heat and mass within the polymer particle is assumed to be negligible.

POLYMERIZATION BY SUPPORTED METALLOCENES

Metal Extraction

When heterogeneous catalysts are considered, it is important to consider the interactions of the metallocene catalyst (and the cocatalyst) with the support structure and its effect, if any, on the polymerization kinetics and on the morphology of the polyolefin particles. Two of the three main routes for metallocene immobilization on supports involve ionic interactions between the metallocene and surface sites of the support or anchored cocatalyst.[19] In these cases, it is possible that the physically sorbed metallocene can be extracted off the support structure during polymerization. For example, Munoz-Escalona et al.[20] have reported the leaching of the metallocene in cases where the metallocene is directly adsorbed over inorganic supports as well as in cases where it is supported on previously passivated supports treated with methylaluminoxane, a common cocatalyst in metallocene systems. Thus, while considering modeling of the particle growth and morphology development during polyolefin synthesis by supported metallocenes, it is necessary to incorporate the effects of metal extraction. Thus, new features need to be incorporated into the MGM described above to model the effects of metal extraction. In both slurry as well as gas phase systems, the metal can be extracted from the support into the swollen polymer phase around the catalyst as shown in Figure 2. In the case of slurry systems, the liquid in the particle pores can extract the catalyst from the polymer and allow it to diffuse out of the particle. In the case of gas phase processes, metal diffuses through the polymer phase in the microparticles and can accumulate on the surface of the microparticles, with possible surface diffusion along the microparticle surface. The metal that collects on the outer surface of the microparticles can catalyze polymerization, leading to the distribution or oozing of polymer into the pores. In addition, when operating condensed mode gas phase reactors, it is possible that capillary condensation of the inerts, diluents, or even the comonomer takes place. If that were to happen, the presence of a liquid in the pores would lead to similar considerations as for slurry systems. It will be shown that the morphological features of polymer particles synthesized using supported metallocene catalysts can be affected by the extraction of active catalyst in both slurry as well as gas phase systems, but particularly so in slurry systems.

The MGM is extended here to model the extraction of the metal and its effect on the kinetics and morphology of the growing polymer particle. Thus, it is necessary to consider the diffusion of metal in a radial direction out of the microparticles and macroparticles (Fig. 2). For traditional Ziegler–Natta catalysts, all reactions occur on the surface of the catalyst fragments within the growing microparticles. However, for physically adsorbed catalysts, extraction of the metal leads to the free metal functioning as a homogeneous catalyst dissolved in the polymer phase surrounding the catalyst fragment and in the liquid in the pores of the polymer particle. In this case, polymerization can occur not only at the surface of the catalyst fragments, but also in the polymer of the microparticles and in the pores of the macroparticle. In addition, for slurry systems, where polymer is present in the pores of the macroparticle, both metal and monomer are assumed to partition between the liquid present and the polymer being formed in the pores.

It should be noted that it is assumed in this discussion that the cocatalyst is present uniformly at all points in the particle, whereby metal on the support as well as the metal extracted out has the same activation and deactivation kinetics. However, it is possible to extend this analysis to cases in which the cocatalyst may be nonuniformly distributed.

Model Assumptions

Other than the usual assumptions made in the modeling of polyolefin particle morphology, using the MGM the following assumptions are made:

(i) The physical picture of the model is shown in Figure 2.

(ii) Metal extraction from the catalyst support into the surrounding polymer phase is governed by extraction equilibrium, and is characterized by the parameter k_{extr}

$$[Me]_{\text{polymer}} = k_{\text{extr}}[Me]_{\text{het}} \tag{1}$$

(iii) In the case of slurry systems, metal diffuses through the polymer phase in the microparticles and is extracted out of the polymer phase into the liquid present in the pores of the particle. The equilibrium relation between metal in the polymer phase and that sorbed to the diluent in the pores gives

$$[Me]_{\text{void}} = k_{\text{sorp,me}}[Me]_{\text{polymer}} \tag{2}$$

For gas phase systems, one could imagine metal accumulating at the outer surface of the microparticles. In the modeling equations developed here, a no flux condition is considered since metal cannot be extracted into the gaseous phase. However, if there is capillary condensation of comonomer or inerts in the pores, then there could be extraction just as in the slurry case, and results from the slurry simulations can in such a case be applied to gas phase systems.

The mass balance equation for the metal in the microparticle ($r_c \le r_s \le R_s$) is written in spherical polar coordinates as:

$$\frac{\partial [Me]_s}{\partial t} = \frac{D_{s,me}}{r_s^2}\frac{\partial\left[r_s^2\dfrac{\partial [Me]_s}{\partial r_s}\right]}{\partial r_s}$$

$$\begin{aligned}
&r_s = r_c && [Me]_s = k_{\text{extr,me}}[Me]_{\text{het}}\\
&r_s = R_s = \phi r_c && [Me]_s = \frac{1}{k_{\text{sorp,me}}}[Me]_{\text{void}} \quad \text{(slurry)}\\
& && \frac{d[Me]_s}{dr_s} = 0 \quad \text{(gas phase)}\\
&t = 0 && [Me]_s = 0
\end{aligned} \tag{3}$$

The radial profile of monomer concentration in the microparticle is then given by

$$\frac{\partial [M_i]_s}{\partial t} = \frac{D_{s,\text{mon}}}{r_s^2}\frac{\partial\left[r_s^2\dfrac{\partial [M_i]_s}{\partial r_s}\right]}{\partial r_s} - (R_p)_i$$

$$\begin{aligned}
&r_s = r_c && 4\pi r_c^2 D_{s,\text{mon}}\frac{\partial [M_i]_s}{\partial r_s} = \frac{4}{3}\pi r_c^3 (R_p)_i^S\\
&r_s = R_s = \phi r_c && [M_i]_s = \eta_{\text{mon}_i}[M_i]_{\text{void}}\\
&t = 0 && [M_i]_s = \eta_{\text{mon}_i}[M_i]^0
\end{aligned} \tag{4}$$

Here, η_{mon_i} represents a Henry's law type of equilibrium relationship between the monomer concentration in the voids and monomer concentration in the polymer. Obviously more complex thermodynamics could be used if desired. As can be seen from eq. (4), reaction takes place not only at the surface of the catalyst fragment (as given by

$(R_p)_i^s$ in the boundary condition at $r_s = r_c$) but also at all points along the radius of the microparticle (as given by $(R_p)_i$) due to the extracted metal. The polymerization rates in the microparticle and at the catalyst fragment surface are:

$$(R_p)_i = k_p[M_i]_s[Me]_s(1 - \bar{C}_{\text{dead}} - \bar{C}_{\text{pot}}) \quad (5a)$$

$$(R_p)_i^S = k_p[Me]|_{\text{het}}[M_i]_s|_{r_c}(E_{\text{cat}} - \bar{C}_{\text{dead}} - \bar{C}_{\text{pot}}) \quad (5b)$$

where E_{cat} is the maximum moles of active sites per mole of metal on the support. It is conceivable that the unsupported catalyst may behave differently from the supported one. For supported catalysts, since some of the metal can be shielded from the monomer due to the support cage, not all of the metal can be activated; thus a value of E_{cat} less than unity is usually observed. However, we assume that all the extracted metal can be activated, thus leading to an increase in productivity upon metal extraction. To avoid confounding the results on porosity and particle morphology caused by the higher activity of the extracted metal, the simulations for slurry systems assume that there is no change in catalyst activity as the metal is extracted from the support (i.e., $E_{\text{cat}} = 1$ for both supported and extracted metal in this case). Thus, changes in properties such as particle porosity or diffusional limitations are compared with catalyst effectiveness the same in each phase. The effect of the enhanced activity of the extracted metal is presented in the case of gas phase systems, where there is no metal extraction into the pores. As will be discussed later, in such a case, with no polymer being formed in the pores, effects on the particle porosity and diffusional limitations are only due to the enhanced catalyst effectivity and consequent higher yields obtained with the extracted homogeneous catalyst.

The concentration of metal and monomer in the pores of the particle at any radial position is a composite of the concentrations in the voids of the pores and the concentration in the polymer present in the pores:

$$[Me]_l = \varepsilon_{\text{void}}[Me]_{\text{void}} + \varepsilon_{\text{pol}}[Me]_{\text{pol}} \quad (6a)$$

$$[Me]_{\text{pol}} = \frac{1}{k_{\text{sorp,me}}}[Me]_{\text{void}} \quad (6b)$$

$$[M_i]_l = \varepsilon_{\text{void}}[M_i]_{\text{void}} + \varepsilon_{\text{pol}}[M_i]_{\text{pol}} \quad (7a)$$

$$[M_i]_{\text{pol}} = \eta_{\text{mon}_i}[M_i]_{\text{void}} \quad (7b)$$

The governing equation for the diffusion of metal in the pores of the macroparticle involves the weighted sum of the diffusive flux through the void spaces in the pores as well as diffusion through the polymer present in the pores:

$$\frac{\partial[Me]_l}{\partial t} = \varepsilon_{\text{void}}\frac{1}{r_l^2}\frac{\partial}{\partial r_l}\left[r_l^2(D_{v,\text{me}})_{\text{eff}}\frac{\partial[Me]_{\text{void}}}{\partial r_l}\right] + \varepsilon_{\text{pol}}\frac{1}{r_l^2}\frac{\partial^2}{\partial r_{l_l}}\left[r_l^2 D_{p,\text{me}}\frac{\partial[Me]_{\text{pol}}}{\partial r_l}\right] + (R_v)_{\text{me}}$$

$$r_l = 0 \qquad \frac{\partial[Me]_l}{\partial r_l} = 0$$

$$r_l = R_l \qquad [Me]_{\text{void}} = [Me]_{\text{bulk}}$$

$$t = 0 \qquad [Me]_{\text{void}} = [Me]_l = 0 \quad (8)$$

where the overall rate of metal flux into the pores ($(R_v)_{me}$) is given by the total flux of metal out of all the microparticles in a given shell:

$$(R_v)_{me} = -\frac{3}{r_c}D_{s,me}\left.\frac{d[Me]_s}{dr_s}\right|_{\phi r_c} \times \frac{(1 - \varepsilon_{\text{void}} - \varepsilon_{\text{pol}})}{\phi} \quad (9)$$

The monomer concentration profile can be similarly written as

$$\frac{\partial[M_i]_l}{\partial t} = \varepsilon_{\text{void}}\frac{1}{r_l^2}\frac{\partial}{\partial r_l}\left[r_l^2(D_{v,\text{mon}_i})_{\text{eff}}\frac{\partial[M_i]_{\text{void}}}{\partial r_l}\right] + \varepsilon_{\text{pol}}\frac{1}{\mathrm{r_l^2}}\frac{\partial}{\partial \mathrm{r_l}}\left[\mathrm{r_l^2 D_{p,mon_i}}\frac{\partial[M_i]_{\text{pol}}}{\partial r_l}\right] - (R_v)_{\text{mon}_i}$$

$$r_l = 0 \qquad \frac{\partial[M_i]_l}{\partial r_l} = 0$$

$$r_l = R_l \qquad [M_i]_{\text{void}} = [M_i]_{\text{bulk}}$$

$$t = 0 \qquad [M_i]_{\text{void}} = [M_i]^0 \quad (10)$$

where the total rate of consumption of monomer at a given radius of the macroparticle can be given as

$$(R_v)_{\text{mon}_i} = [\varepsilon_{\text{cat}}(R_p)_i^S + \varepsilon_s(R_p)_{i,\text{ave}}] + [\varepsilon_{\text{void}}(R_p)_{i,\text{void}} + \varepsilon_{\text{pol}}(R_p)_{i,\text{pol}}] \quad (11)$$

The terms in the second bracket are applicable only for slurry systems (or other systems where there may be liquid in the pores) as they account for reaction taking place in the pores (in the void space and in the polymer phase present in the pores) of the macroparticle. The average rate of reaction in all the microparticles in a given macroshell, is given by

$$(R_p)_{i,\text{ave}} = \frac{\int_{r_c}^{\phi r_c} 4\pi r^2 (R_p)_i dr}{\int_{r_c}^{\phi r_c} 4\pi r^2 dr} \tag{12}$$

while the reaction rates in the voids and in the polymer of the pores are

$$(R_p)_{i,\text{void}} = k_p[Me]_{\text{void}}[M_i]_{\text{void}}(1 - \bar{C}_{\text{dead}} - \bar{C}_{\text{pot}}) \tag{13a}$$

$$(R_p)_{i,\text{pol}} = k_p[Me]_{\text{pol}}[M_i]_{\text{pol}}(1 - \bar{C}_{\text{dead}} - \bar{C}_{\text{pot}}) \tag{13b}$$

The macroparticle diffusivities in the above equation are obtained from the bulk diffusivity of the species in the liquid/gas, corrected by the void fraction and a tortuosity factor.

$$(D_{v,i})_{\text{eff}} = D_{b,i}\frac{\varepsilon_{\text{void}}}{\tau} \qquad i = \text{me, mon} \tag{14}$$

The microparticle diffusivities and diffusivity through the polymer in the pores are obtained from the Michaels and Bixler correlation[21] by considering diffusion through the amorphous polymer.

$$D_{p,i} = D_{s,i} \qquad i = \text{me, mon} \tag{15}$$

The rate of change of metal concentration on the support is calculated by considering the flux of metal diffusing out of the catalyst fragment surface at any time

$$\frac{d[Me]_{\text{het}}}{dt} = \frac{3}{r_c} D_{s,\text{me}} \left.\frac{d[Me]_s}{dr_s}\right|_{r_c}$$

$$\text{Initial condition: } t = 0 \qquad [Me]^0_{\text{het}} = \frac{w_{\text{me}}\rho_{\text{cat}}}{\text{MW}_{\text{me}}} \tag{16}$$

where w_{me} is the weight fraction of metal on the catalyst (grams of metal/gram of catalyst), ρ_{cat} is the catalyst density, and MW_{me} is the molecular weight of the metal.

Excessive particle temperatures also can cause particle sintering with reductions in particle porosity and increased diffusion limitations in the particle.[22,23] However, we will assume an isothermal particle in the present study.

The quasi-steady-state assumption (QSSA) can be made for microparticle diffusion of the metal and monomer since the time constant for monomer/metal concentration to reach a quasi-steady-state value in the microparticle is of the order of a fraction of a second to a few seconds, at most. Finite difference methods are used to compute the macroparticle and microparticle monomer concentration profiles. The macroparticle model equations are solved for N_l shells at varying radial distances in the macroparticle. The method of solution is similar to that described by Hutchinson and Ray[6] and Debling and Ray,[7] with the complete set of discretized macroparticle and microparticle mass balances and corresponding sets of catalyst site balances sent to a differential-algebraic system equation solver (DASSL).[24] The microparticle growth factor, φ, which is estimated from the sum of the volume of polymer formed at the catalyst fragment surface ($V_{\text{pol},1}$) and the volume of polymer formed by the extracted metal in the polymer phase surrounding the catalyst fragment ($V_{\text{pol},2}$) is used to update the grid positions. In slurry systems, the total volume of polymer formed in the pores ($V_{\text{pol,pore}}$) is used to compute ε_{pol}, the fraction of shell volume occupied by the polymer in the pores. Thus, the volume of polymer formed at the (heterogeneous) catalyst surface (cm^3 of polymer/cm^3 of catalyst) is calculated as

$$\frac{dV_{\text{pol},1}}{dt} = \frac{\sum_{i=1}^{N\text{Mon}} (R_p)_i^S \,\text{MW}_{M_i}}{\rho_{\text{pol}}}$$

$$\text{Initial condition: } t = 0 \qquad V_{\text{pol},1} = (\phi^0)^3 - 1 \tag{17}$$

The volume of polymer formed by the extracted metal in the microparticles (cm^3 of polymer/cm^3 of amorphous polymer in the microparticles) is calculated by summing the total polymer formed due to reaction at each micro-radius within a microparticle:

$$\frac{dV_{\text{pol},2}}{dt} = \frac{\sum_{i=1}^{N\text{Mon}} (R_p)_{i,\text{ave}} \text{MW}_{M_i}}{\rho_{\text{pol}}}$$

$$\text{Initial condition: } t = 0 \qquad V_{\text{pol},2} = 0 \qquad (18)$$

The volume of polymer formed in the pores is given by the sum of the polymer formed in the voids and that formed in the polymer present in the pores:

$$\frac{dV_{\text{pol,pore}}}{dt} = \frac{\sum_{i=1}^{N\text{Mon}} (R_p)_{i,\text{void}} V_{\text{void}} \text{MW}_{M_i}}{\rho_{\text{pol}}} + \frac{\sum_{i=1}^{N\text{Mon}} (R_p)_{i,\text{pol}} \alpha V_{\text{pol,pore}} \text{MW}_{M_i}}{\rho_{\text{pol}}}$$

$$\text{Initial condition: } t = 0 \qquad V_{\text{pol,pore}} = 0 \qquad (19)$$

In order to compute the void fraction across the macroparticle radius, it is assumed that the spatial arrangement of microparticles within the growing particle does not change. A volume balance over the shell, taking into account the different microparticle growth rates and the polymer formed in the pores, is used to compute the variable void fraction across the macroparticle radius.

Slurry Systems

Under the QSSA assumption, eq. (3) can be solved for slurry systems to obtain the following analytic solution for the metal concentration profile in the microparticle:

$$[Me]_s = \frac{\frac{1}{k_{\text{sorp,me}}}[Me]_l - \frac{1}{\varphi} k_{\text{extr}}[Me]_{\text{het}}}{1 - \frac{1}{\varphi}} - \frac{\frac{1}{k_{\text{sorp,me}}}[Me]_l - k_{\text{extr}}[Me]_{\text{het}}}{1 - \frac{1}{\varphi}} \left[\frac{r_c}{r_s}\right] = A + \frac{B}{r_s} \qquad (20)$$

where ϕ is the microparticle growth factor, which can be estimated from a mass balance of polymer produced per microparticle. The flux of metal out of all the microparticles gives the total metal extracted into the pores in a given shell. Using the QSSA assumption and substituting eq. (20) for the metal concentration profile in the microparticle, the microparticle monomer balance [eq. (4)] becomes

$$\frac{D_{s,\text{mon}_i}}{r_s^2} \frac{\partial \left[r_s^2 \frac{\partial [M_i]_s}{\partial r_s} \right]}{\partial r_s} - k_p (1 - \bar{C}_{\text{dead}} - \bar{C}_{\text{pot}}) [M_i]_s \left(A + \frac{B}{r_s} \right) = 0$$

$$r_s = r_c \qquad \frac{\partial [M_i]_s}{\partial r_s} = \frac{r_c}{D_{s,\text{mon}_i}} k_p (E_{\text{cat}} - \bar{C}_{\text{dead}} - \bar{C}_{\text{pot}}) \times [M_i]_s|_{r_c} k_{\text{extr}} [Me]_{\text{het}}$$

$$r_s = R_s = \phi_0 r_c \qquad [M_i]_s = \eta_{\text{mon}_i} [M_i]_{\text{void}} \qquad (21)$$

In order to obtain the microparticle monomer profile, the spatial derivative is discretized using finite differences into N_s micro-shells within each of the macro-shells. An analytical solution is also possible in terms of confluent hypergeometric functions, with the solution rendered as a sum of Whittaker functions.[25] However, the evaluation of these functions is more computationally intensive and complicated, and hence the numerical solution based on a finite-difference discretization is used here.

Gas Phase Systems

For gas phase systems, an analytic solution can be derived for both monomer and metal microparticle profiles. The total metal within a microparticle at any time is a constant, since a no flux condition is considered at the outer edge. Thus a volume balance for the metal gives us the amount of metal at any micro-radius (constant profile across the microparticle due to the QSSA assumption):

$$[Me]_s = k_{\text{extr}} [Me]_{\text{het}} = k_{\text{extr}} \frac{[Me]^0_{\text{het}}}{1 + \alpha k_{\text{extr}} (\phi^3 - 1)} \qquad (22)$$

The transport equation for the monomer in the microparticle then reduces to the form of the clas-

sic equation for diffusion with first order reaction, and can be solved analytically. Thus, eq. (21) becomes:

$$\frac{1}{r_s^2}\frac{\partial\left[r_s^2\dfrac{\partial[M_i]_s}{\partial r_s}\right]}{\partial r_s} = \Lambda^2[M_i]_s$$

$$r_s = r_c \qquad \frac{\partial[M_i]_s}{\partial r_s} = \frac{r_c}{3D_{s,\mathrm{mon}_i}} k_p(E_{\mathrm{cat}} - \bar{C}_{\mathrm{dead}} - \bar{C}_{\mathrm{pot}}) \times [Me]_{\mathrm{het}}[M_i]_s|_{r_c}$$

$$r_s = R_s = \phi_0 r_c \qquad [M_i]_s = \eta_{\mathrm{mon}_i}[M_i]_{\mathrm{void}} \tag{23}$$

where

$$\Lambda^2 = \frac{k_p(1 - \bar{C}_{\mathrm{dead}} - \bar{C}_{\mathrm{pot}})k_{\mathrm{extr}}}{D_{s,\mathrm{mon}_i}} \frac{[Me]^0_{\mathrm{het}}}{1 + \alpha k_{\mathrm{extr}}(\phi^3 - 1)} \tag{24}$$

The solution, which gives the monomer concentration profile across the microparticle radius, can be then given in the form:

$$[M_i]_s = c_1\frac{\cosh(\Lambda r_s)}{r_s} + c_2\frac{\sinh(\Lambda r_s)}{r_s} \tag{25}$$

where the boundary conditions give the values of c_1 and c_2.

$$c_1 = \frac{\eta_{\mathrm{mon}_i}[M_i]_{\mathrm{void}}\left(\dfrac{\Lambda\cosh(\Lambda r_c)}{r_c} - \dfrac{\sinh(\Lambda r_c)}{(r_c)^2}\right) - \dfrac{r_c}{3D_{s,\mathrm{mon}_i}} \times k_p(E_{\mathrm{cat}} - \bar{C}_{\mathrm{dead}} - \bar{C}_{\mathrm{pot}})[Me]_{\mathrm{het}}[M_i]_s|_{r_c}\dfrac{\sinh(\Lambda\phi r_c)}{\phi r_c}}{\dfrac{\cosh(\Lambda\phi r_c)}{\phi r_c}\left(\dfrac{\Lambda\cosh(\Lambda r_c)}{r_c} - \dfrac{\sinh(\Lambda r_c)}{(r_c)^2}\right) - \left(\dfrac{\Lambda\sinh(\Lambda r_c)}{r_c} - \dfrac{\cosh(\Lambda r_c)}{(r_c)^2}\right)\dfrac{\sinh(\Lambda\phi r_c)}{\phi r_c}} \tag{25a}$$

$$c_2 = \frac{\dfrac{r_c}{3D_{s,\mathrm{mon}_i}} k_p(E_{\mathrm{cat}} - \bar{C}_{\mathrm{dead}} - \bar{C}_{\mathrm{pot}})[Me]_{\mathrm{het}}[M_i]_s|_{r_c}\dfrac{\cosh(\Lambda\phi r_c)}{\phi r_c} - \eta_{\mathrm{mon}_i}[M_i]_{\mathrm{void}}\left(\dfrac{\Lambda\sinh(\Lambda r_c)}{r_c} - \dfrac{\cosh(\Lambda r_c)}{(r_c)^2}\right)}{\dfrac{\cosh(\Lambda\phi r_c)}{\phi r_c}\left(\dfrac{\Lambda\cosh(\Lambda r_c)}{r_c} - \dfrac{\sinh(\Lambda r_c)}{(r_c)^2}\right) - \left(\dfrac{\Lambda\sinh(\Lambda r_c)}{r_c} - \dfrac{\cosh(\Lambda r_c)}{(r_c)^2}\right)\dfrac{\sinh(\Lambda\phi r_c)}{\phi r_c}} \tag{25b}$$

Polymer Compressibility

The use of single-site metallocene catalysts has made it possible to obtain polyolefins with narrow molecular weight distributions (MWD), narrow chemical compositional distributions (CCD), more uniform sequence length distribution, and higher comonomer incorporation. Because of these unique features, it has been observed that the properties and morphology of these polymers are very different than those obtained under similar reaction conditions with traditional Ziegler–Natta catalysts. In particular, the narrow chemical composition distribution and more uniform sequence length distribution leads to the synthesis of polymers with lower melting points than those produced using traditional Ziegler–Natta catalysts. For example, Furtek[2] reported lower melting points for LLDPE synthesized using a metallocene cocatalyst compared with that produced with a commercial Ziegler catalyst, even though both polymers had the same density (0.918 g/cm^3). Nascent polymer melting points 10–20°C lower for metallocene polymers are widely reported. It has also been reported that the polymer crystallite sizes are smaller in the case of metallocene polymers. For example, Churdpunt and Isayev[26] reported lower melting points for metallocene-based isotactic polypropylene compared with the Ziegler–Natta catalyst product. At the same molecular weight, the rate of crystallization and spherulitic growth rates were lower for the metallocene-based polymer, with a much smaller spherulite size. In the case of polypropylene resins, Bond and Spruiell[27] suggest that the crystalline lamellae produced by the metallocene catalysts are not as stable as the lamellae produced by Ziegler–Natta, causing a lowering of the melting point. Figure 3 compares the morphology of a resin particle for the two catalyst systems. The metallocene polymer is found to be much denser, with very little porosity. In light of these and other experimental observations, it is possible that in the case of a metallocene polymer, the lower melting point produces softer and more

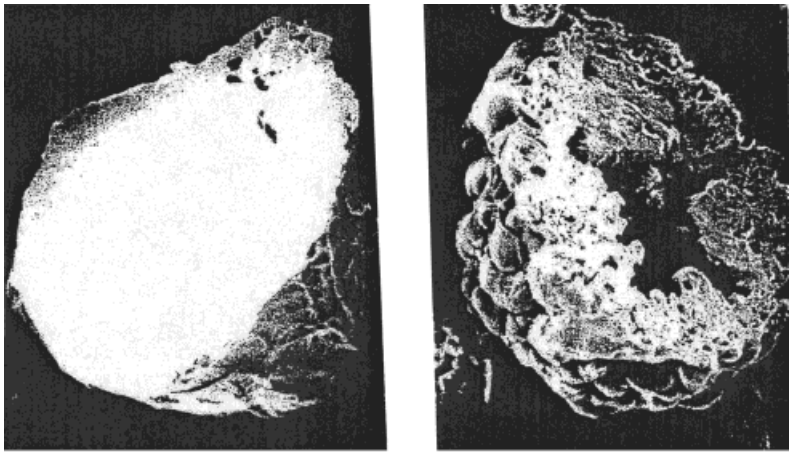

Figure 3 Comparison of morphology of polyolefin particles synthesized from a metallocene catalyst and from a traditional Ziegler–Natta catalyst.[2]

compressible polymer microparticles. This means that as the macroparticles grow, the enormous pressures required to expand the particle cause the softer metallocene polymer microparticles to deform rather than rigidly to grow larger (cf. Fig. 4).

Here, this compression of the microparticles has been modeled within the framework of the MGM by defining a compressibility factor as used previously[7] to model decreasing particle porosity with increasing polymer yield. A geometric correlation is used to compute the microparticle compressibility factor (z), which gives the diameter of the compressed microparticle (perpendicular to the radial coordinate) with respect to that of a perfect sphere:

$$z = 1 - \beta(\phi - 1)^n \tag{26}$$

where β and n are user-specified coefficients. As discussed earlier, a volume balance over the shell, taking into account the different microparticle growth rates and the polymer formed in the pores, is used to compute the variable void fraction across the macroparticle radius. The effects of variable void fraction and microparticle compressibility are incorporated into the MGM model by updating the grid positions along the particle radius based on the growth factor and the compressibility coefficient at that radius. Thus, the position of grid point r_n for a given macroshell (n) can be calculated using the constant spatial position assumption as

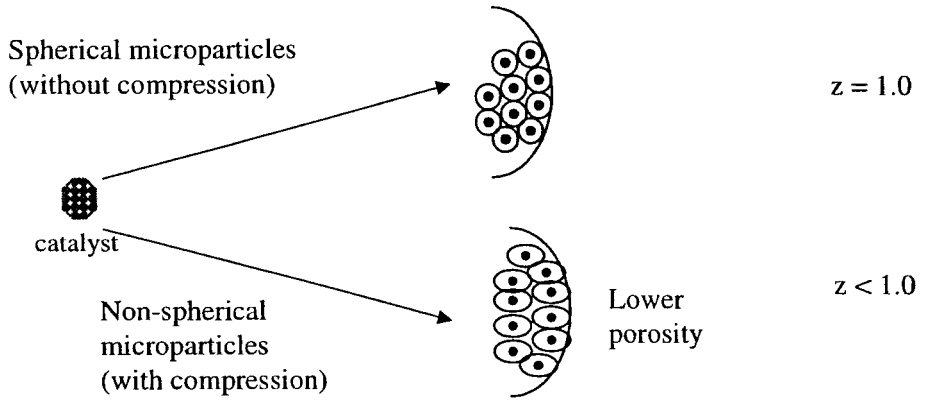

Figure 4 Compressibility of microparticles.

Table I General Kinetic Scheme for Olefin Polymerization

	Site Activation	Chain Initiation	Propagation	Chain Transfer	Site Transformation	Site Deactivation	TDB Formation
Hydrogen	●			●	●	●	
Cocatalyst	●			●	●	●	
Electron donor	●			●	●	●	
Solvent				●	●		
Transfer agent				●			
Inhibitor					●	●	
Byproduct						●	
Spontaneous	●			●	●	●	●
Monomer(s)	●	●	●	●	●	●	●

(●) Reactions that are possible and that can be considered in the kinetic scheme.

$$r_n = r_{n0}\phi_n z_n \tag{27}$$

Typical values for β and n are 1.25×10^{-6} and 3, respectively. Varying the value of β, it is possible to model different levels of microparticle compressibility and to study the effects on polymer morphological features such as porosity and on the kinetics and mass transfer limitations within the polymer macroparticle.

RESULTS AND DISCUSSION

Effects of Metal Extraction

The results are presented for the case of propylene homopolymerization catalyzed by a single site metallocene catalyst. The particle model and simulation results, however, would apply equally well to the copolymerization of other monomers with metallocene catalysts. A general kinetic scheme for olefin polymerization has been discussed by Chen[28] and Shaffer and Ray.[29] This kinetic scheme (summarized in Table I) accounts for multiple active sites, with each active site having its own kinetic scheme involving activation, deactivation, site transformation, chain transfer, propagation, as well as internal and terminal double bond reactions. In the present study, only site activation, propagation, and site deactivation are considered for a single-site metallocene catalyst. The detailed kinetic model will be used in a future publication to evaluate the effects of metal extraction and simultaneous heterogeneous and homogeneous polymerization on polymer properties, MWD broadening, and compositional heterogeneity. Parameters used in the simulations are summarized in Table II.

The site balance equations for the chosen kinetic scheme are given by eqs. (28)–(30), where the concentrations of sites, expressed on a frac-

Table II Stimulation Model Parameters

Catalyst parameter
- R_L ($t = 0$): 25 μm (macroparticle)
- r_c: 0.01 μm (microparticle)
- 2 wt % metal loading ($w_{me} = 0.02$)
- $\rho_{\text{cat}} = 2.33$ g/cm^3
- $\varepsilon_{\text{void}}(t = 0)$: 0.25
- $\text{MW}_{me} = 47.9$
- Catalyst activity: 12,000 g PP/(g cat h) at $[\text{M}]_{\text{bulk}}$ of 2 mol/L (slurry)

Gas phase
- Pressure: 20 atm, temperature: 70°C
- $\Delta H_p = -25{,}500$ cal/mole

Sorption factor for propylene
- $\eta_{mon} = 0.5$ (polymer/liquid)
- $\eta_{mon} = 1.52$ (polymer/gas):

Amorphous fraction of polymer, $\alpha = 0.37$

Bulk diffusivity through liquid (cm^2/s): $D_{b,\text{me}}$: 1.6×10^{-6}
$D_{b,\text{mon}}$: 4.2×10^{-6}

Bulk diffusivity through gas (cm^2/s): $D_{b,\text{mon}}$: 0.45×10^{-2}

Diffusivity through polymer phase (cm^2/s): $D_{s,\text{me}}$: 1×10^{-13}
$D_{s,\text{mon}}$: 1.3×10^{-7}

Tortuosity factor, $\tau = 6.0$

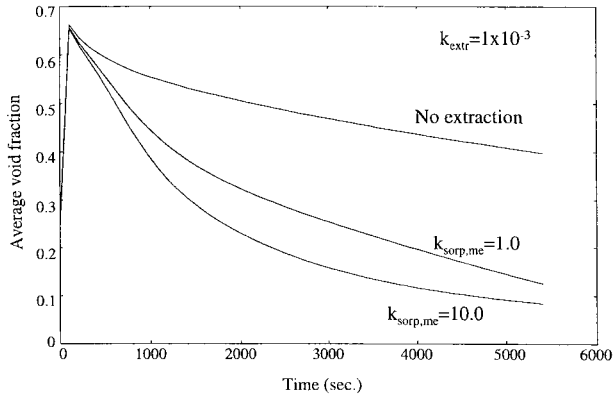

Figure 5 Slurry systems. Effect of metal extraction on average particle porosity.

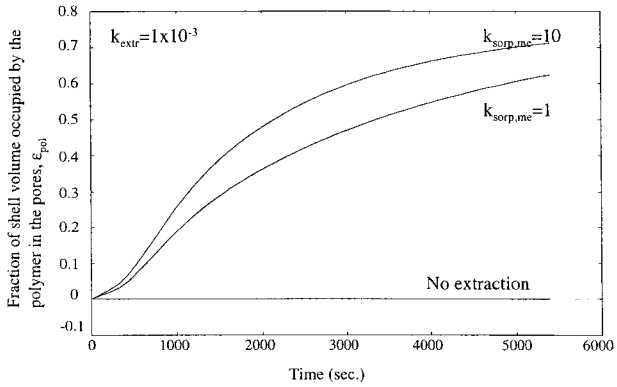

Figure 6 Slurry systems. Fraction of shell volume occupied by the polymer in the pores.

tional basis, are normalized by the total amount of active metal in the catalyst and have units of moles/ mole of metal. Thus, fractional dead site concentration (moles dead site/mole metal) is given as

$$\frac{d\bar{C}_{\text{dead}}}{dt} = k_{d_0}\exp\left(-\frac{E_d}{RT}\right)\bar{C}_{\text{act}}$$

$$\text{Initial condition: } t = 0 \qquad \bar{C}_{\text{dead}} = 0 \qquad (28)$$

and the fractional potential site concentration (moles potential sites/ mole metal) is

$$\frac{d\bar{C}_{\text{pot}}}{dt} = k_{a0}\exp\left(-\frac{E_a}{RT}\right)\bar{C}_{\text{pot}}$$

$$\text{Initial condition: } t = 0 \qquad \bar{C}_{\text{pot}} = 0.2xE_{\text{cat}} \qquad (29)$$

For the single site metallocene catalyst, the fractional active site concentration (moles active sites/ mole metal) is found from the values obtained from eqs. (28) and (29) for the dead site and potential site concentrations, respectively, as

$$\bar{C}_{\text{act}} = E_{\text{cat}} - \bar{C}_{\text{dead}} - \bar{C}_{\text{pot}} \qquad (30)$$

Slurry Systems

As discussed above, polymerization occurs not only because of the heterogeneous catalyst but because of the homogeneous catalyst extracted into the polymer phase and into the pores of the particle as well. This leads to a lowering of the porosity of the particle with time, as polymer is formed in the pores. Figure 5 shows the effect of $k_{\text{sorp,me}}$ on the void fraction of the polymer particle. Since $k_{\text{sorp,me}}$ governs the amount of metal extracted into the pores, a higher value of $k_{\text{sorp,me}}$ lead to greater amounts of polymer being formed in the pores (Fig. 6), giving a polymer particle with very low porosity (Fig. 5). Figure 7 shows that as metal diffuses out of the supported catalyst, the fraction of polymer formed at the heterogeneous catalyst sites decreases, with polymer also being formed in the polymer phase of the microparticles and in the pores by the extracted homogeneous catalyst. A difference in the characteristics and properties of the active metal sites, depending on whether it was on the support or in the polymer/pore phases, can have a direct impact on polymer properties, possibly leading to MWD broadening and compositional heterogeneity (in copolymer systems). These effects will be discussed in a later publication, when additional

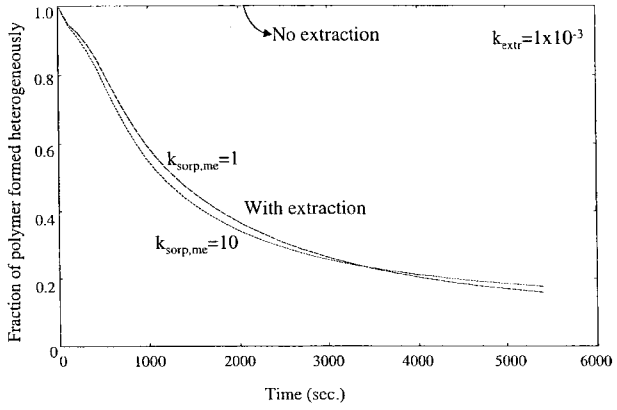

Figure 7 Slurry systems. Fraction of polymer formed by the heterogeneous (supported) catalyst.

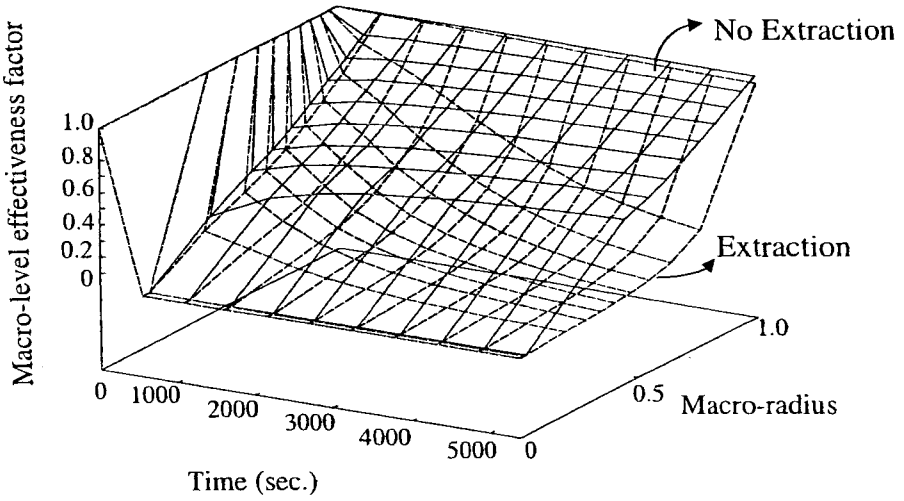

Figure 8 Slurry systems. Monomer macroparticle diffusional limitation, with and without metal extraction.

experimental information is available on these differences in the supported and extracted metal. The role of the cocatalyst and its interaction with the support also needs to be investigated thoroughly.

As the macroparticle pore volume fills up with polymer, lowering the porosity and pore volume, monomer diffusional limitations in the macroparticle can arise, lowering the rate of polymerization. As a comparison of pure heterogeneous catalysis versus the case with catalyst extraction, Figure 8 shows the extent to which diffusional limitations in the polymer particle are aggravated by the formation of polymer in the pores. Since diffusion of monomer through the polymer phase is much slower than through the liquid phase, this can lead to a pore plugging effect, with more polymer formed in pores on the outside of the particle due to a steep gradient in monomer concentration within the particle. Thus, in the extreme case, hollow polymer particles can even be expected.

Gas Phase Systems

In the case of gas phase systems, since all the metal is present within the confines of the growing microparticles at any time, considering the same catalyst activity for both the supported and the extracted metal gives us identical morphology and porosity profiles. The catalyst activity can be defined in terms of the maximum number of moles of active sites per mole of metal (E_{cat}). In the case of supported catalysts, this value is less than unity, since not all the metal atoms can be activated due to shielding of some of the metal atoms due to the support cage structure. In such a case, the extracted metal ($E_{cat} = 1$) has a higher activity than that of the supported metal.

Thus, metal extraction leads to a system with higher overall activity of the catalyst, resulting in higher yields, greater degree of compression of the microparticles at these yields, and lowered porosity (Fig. 9). However, this effect is only attributable to the enhanced activity of the extracted metal and not to any direct or indirect physical effect of the extraction process. Thus, in gas phase systems, unless there is condensation of diluents or comonomers in the pores, extraction of metal only has an effect on particle morphology owing to the differences in activity and properties of the extracted metal from the supported metal. In case there is a liquid phase in the pores due to capillary condensation, similar considerations as in the slurry case hold. Thus, in that case, it is necessary to consider extraction of metal into the pores and subsequent decrease in porosity of the particle due to the formation of polymer in the pores.

Effect of Microparticle Compressibility

The effect of the microparticle compressibility is to cause rapidly decreasing particle porosity with increasing polymer yield. As discussed before, be-

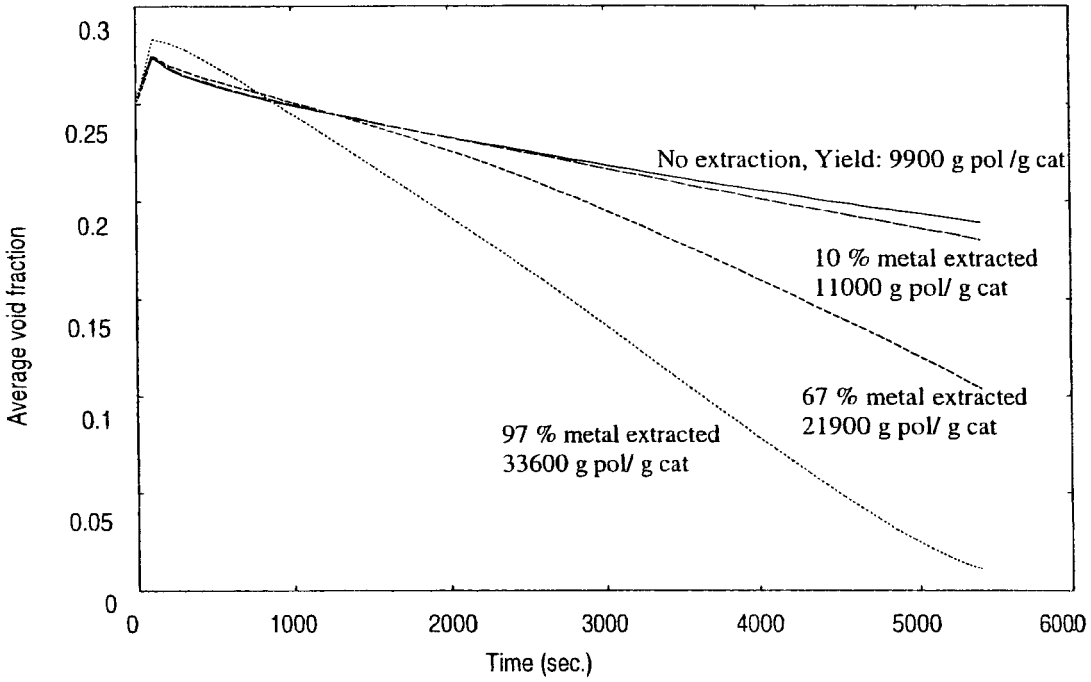

Figure 9 Gas phase systems. Effect of higher reactivity of the extracted metal on particle porosity.

cause of the unique properties of the polymer formed using a single-site metallocene catalyst, it is possible to get softer polymer particles. Thus, the microparticles are compressed during the growth of the polymer particle to a greater extent than in Ziegler–Natta synthesized polyolefins. This compression of the microparticles can be modeled within the framework of the MGM model by considering the variation in the compressibility coefficient, z, in eq. (26). Thus, in order to study the impact of higher compressibilities of the metallocene polymers on the porosity of the particle, the parameter β is varied. Figure 10 shows a drastic effect of the polymer compressibility on the particle porosity. Note that higher values of β lead to a lower value for the compressibility factor z, i.e., higher compressibilities. This decrease in polymer porosity has a direct effect on the monomer accessible within the particle. Figure 11

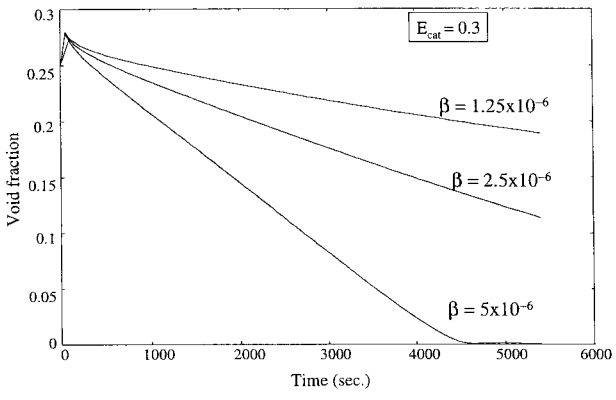

Figure 10 Effect of compressibility of microparticles on particle void fraction.

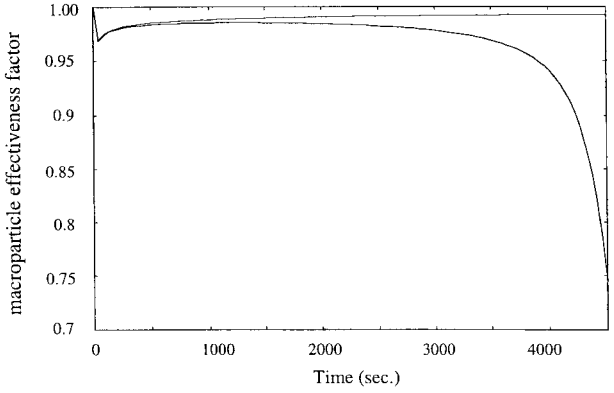

Figure 11 Effect of compressibility of microparticles on macroparticle diffusional limitations to monomer transport.

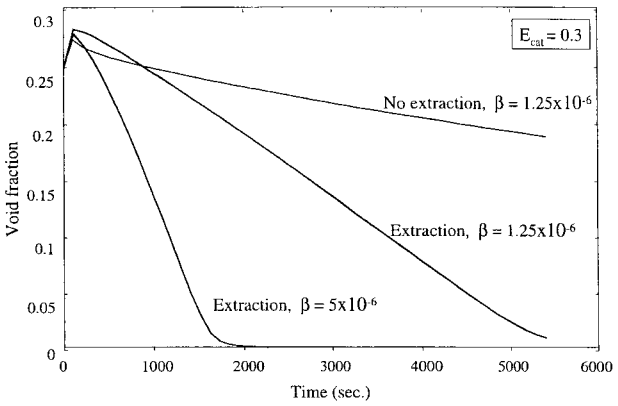

Figure 12 Combined effect of compressibility of microparticles and metal extraction on particle void fraction.

shows the effect of higher compressibility and lowered porosity on the macroparticle effectiveness factor for the diffusing monomer. Thus, it can be seen that the use of supported metallocenes can lead to more compressible particles, which in turn leads to lowered porosity and the possibility of increased mass transfer limitations for monomer diffusion. When this is accompanied by metal extraction, the lowering of porosity and the aggravation of diffusional limitations to monomer transport into the particle are even greater. Figure 12 compares the combined effect of higher compressibility and metal extraction in a gas phase system with a case with no metal extraction.

These results show that it is possible to obtain polymer particles with very low porosities due to the effects of metal extraction and the synthesis of softer, more compressible polymer. The model simulations are in good qualitative agreement with experimentally observed results.[1,2]

SUMMARY

It is clear that a wide variety of porosity profiles for polyolefin particles can be predicted using the MGM. Figure 13 presents a schematic of the typical porosity profiles that can be expected as a result of various physical processes. The MGM can predict all these cases, in agreement with observed experimental data. However, further modeling and experimental work is required to fully understand and control polymer morphology with supported metallocenes. It is well known that the adsorption of the organometallic species onto inorganic surfaces can also alter their reactivities and catalytic activities. This needs to be explored further. In addition, the effects of extracted or separately added cocatalyst require further study. A future communication will deal with the effect of metal extraction on polymer

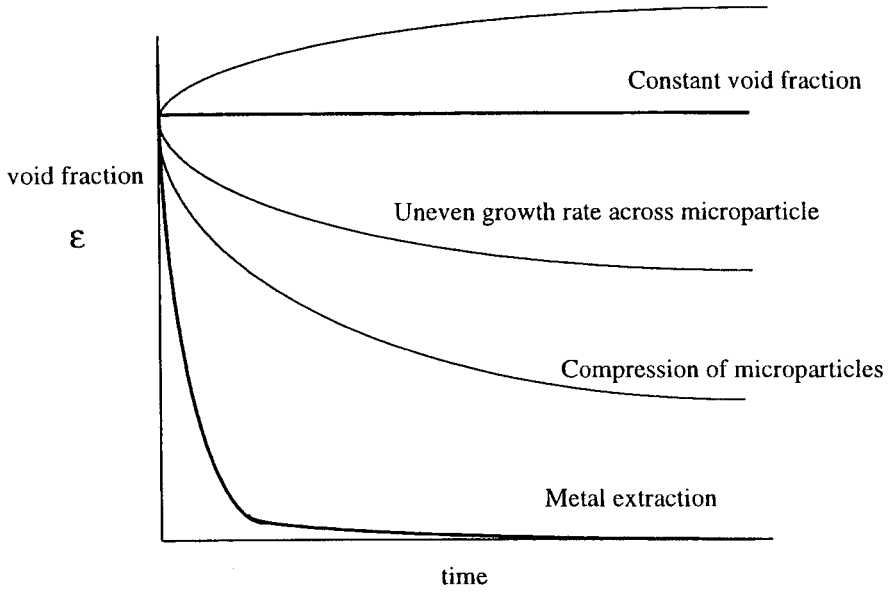

Figure 13 Schematic of possible porosity profiles in olefin polymerization.

properties such as MWD broadening, and compositional heterogeneity arising from metal extraction and simultaneous heterogeneous/ homogenous polymerization.

REFERENCES

1. Hoel, E. L.; Cozewith, C.; Bryne, G. D. Adv Inorg Chem 1994, 40, 1669.
2. Furtek, A. B. Ultra Strength Polyethylene Resins Produced in a Fluid-Bed Process Utilizing Metallocene-Based Catalysts, MetCon '93; Houston, TX, 1993.
3. Nagel, E. J.; Kirillov, V. A.; Ray, W. H. Ind Eng Chem Prod Res Dev 1980, 19, 372.
4. Taylor, T. W.; Choi, K.-Y.; Yuan, H.-G.; Ray, W. H. In Transition Metal Catalyzed Polymerization; Quirk, R. P., Ed. Harwood Publishers: New York, 1983; p 191.
5. Ray, W. H. In Transition Metal Catalyzed Polymerization: Ziegler–Natta and Metathesis Polymerization; Cambridge University Press: New York, 1989; p 563.
6. Hutchinson, R. A.; Chen, C. M.; Ray, W. H. J Appl Polym Sci 1992, 44, 1389.
7. Debling, J. A.; Ray, W. H. Ind Eng Chem Res 1995, 34, 3466.
8. Kakugo, M.; Sadatoshi, H.; Yokoyama, M.; Kojima, K. Macromolecules 1989, 22, 547.
9. Kakugo, M.; Sadatoshi, H.; Sakai, J.; Yokoyama, M. Macromolecules 1989, 22, 3172.
10. Kakugo, M.; Sadatoshi H.; Sakai, J. In Catalytic Olefin Polymerization, Keii, T., Soga, K., Eds.; Elsevier: New York, 1990; p 345.
11. Simonazzi, T.; Ceechin G.; Mazzullo S. Prog Polym Sci 1991, 16, 303.
12. Galli, P.; Collina, G.; Sgarzi, P., Baruzzi, G.; Marchetti E. J Appl Polym Sci 1997, 66, 1831.
13. Galli, P., Proceedings of the Sixth International Workshop on Polymer Reaction Engineering; DECHEMA: Berlin, 1998; p 61.
14. Floyd, S.; Choi, K. Y.; Taylor, T. W.; Ray W. H. J Appl Polym Sci 1986, 31, 2231.
15. Floyd, S.; Choi, K. Y.; Taylor, T. W.; Ray, W. H. J Appl Polym Sci 1986, 32, 2935.
16. Floyd, S.; Hutchinson, R. A.; Ray, W. H. J Appl Polym Sci 1986, 32, 5451.
17. Floyd, S.; Heiskanen, T.; Taylor, T. W.; Mann, G. E.; Ray W. H. J Appl Polym Sci 1987, 33, 1021.
18. Debling, J. A.; Ray W. H. Proceedings of the Sixth International Workshop on Polymer Reaction Engineering; DECHEMA: Berlin, 1998; p 93.
19. Ribeiro, M. R.; Deffleux, A.; Portela, M. F. Ind Eng Chem Res 1997, 36, 1224.
20. Munoz-Escalona, A.; Mendez, L.; Pena, B.; Lafuente, P.; Sancho, J.; Michiels, W.; Hidalgo, G.; Martinez-Nunez, M. In Metallocene Technology in Commercial Applications; Benedikt, G. M., Ed.; Society of Plastics Engineers: New York, 1999; p 1.
21. Hutchinson, R. A.; Ray, W. H.. J Appl Polym Sci 1990, 41, 51.
22. Han-Adebekun, G. C.; Hamba, M.; Ray, W. H.. J Polym Sci A Polym Chem 1997, 35, 2063.
23. Hamba, M.; Han-Adebekun, G. C.; Ray , W. H. J Polym Sci A Polym Chem 1997, 35, 2075.
24. Brenan K. E.; Campbell, S. L.; Petzold, L. R. Numerical Solution of Initial-Value Problems in Differential-Algebraic Equations; Elsevier Science: New York, 1989.
25. Abramowitz, M.; Stegun, I. A. Handbook of Mathematical Functions, with formulas, graphs, and mathematical tables, 1972.
26. Churdpunt Y.; Isayev, A. I. In Metallocene Technology in Commercial Applications; Benedikt, G. M., Ed.; Plastics Design Library: New York, 1999; p 247.
27. Bond, E. B.; Spruiell, J. E. In Metallocene-Catalyzed Polymers: Materials, Properties, Processing and Markets; Benedikt, G. M., Goodall, B. L., Eds., Plastics Design Library: New York, 1998; p 157.
28. Chen, C. Gas phase olefin copolymerization with Ziegler–Natta catalysts; Ph.D. Thesis, University of Wisconsin, 1995.
29. Shaffer, W. K. A.; Ray, W. H. J Appl Polym Sci 1997, 65, 1053.